MOLECULAR STATE EVOLUTION AFTER EXCITATION WITH AN ULTRA-SHORT LASER PULSE: A QUANTUM ANALYSIS OF NaI AND NaBr DISSOCIATION

Volker ENGEL, Horia METIU

Department of Chemistry, University of California, Santa Barbara, CA 93106, USA

Raphael ALMEIDA, R.A. MARCUS and Ahmed H. ZEWAIL

Arthur Amos Noyes Laboratory of Chemical Physics, California Institute of Technology, Pasadena, CA 91125, USA

Received 28 July 1988; in final form 20 September 1988

In recent experiments Rose, Rosker and Zewail have used a femtosecond pulse to dissociate NaI and NaBr, and a second pulse to probe the "transition state" by LIF. Here we show that quantum calculations, on a model system with no adjustable parameters, reproduce the principal observed features.

1. Introduction

In a recent experiment, Rose, Rosker and Zewail [1,2] used a very short laser pulse to initiate the photodissociation of gaseous NaI and NaBr. The time evolution of the state created by this pulse was monitored by exciting the Na atoms with a delayed probe pulse of different colors and measuring their laser-induced fluorescence (LIF). When the probe pulse is tuned on resonance with the 589 nm sodium D line, LIF probes the population of the free Na atoms; off-resonance excitation probes the population of the Na atoms still trapped in the "transition state" [Na...I].

The dependence of the number of LIF photons on the delay time between the pulses (fig. 1) shows a striking damped, oscillatory behavior. The frequency of the oscillations and the damping time have been related [1,2] to the oscillation frequency in the classical motion of a narrow wave packet in the well of the upper bound state and to the Landau–Zener probability of escaping out of the well. The bound state involved in this process is the upper adiabatic state created by the interaction between the ionic and the neutral states.

For many reasons, both experimental and theoretical, NaBr and NaI offer a unique opportunity to

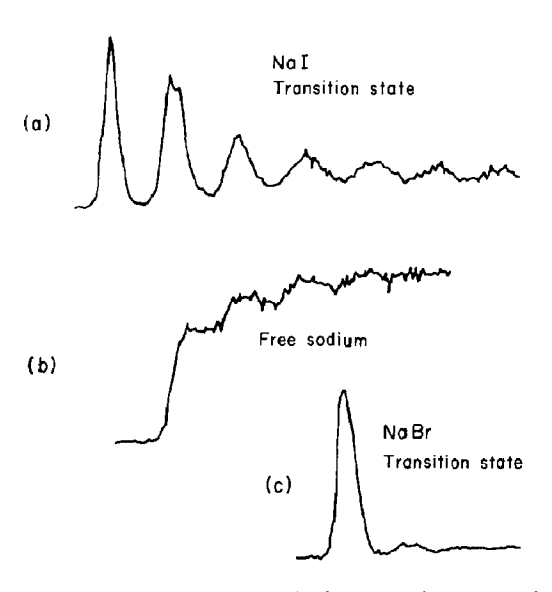


Fig. 1. The experimental results of ref. [1] showing the LIF signal versus the delay time of the probe pulse (the time scale is shown in fig. 3). (a) The probe pulse was tuned to the TS region, off-resonant to the Na D line. (b) The probe pulse was on-resonance with the Na D line. (c) The probe pulse was tuned to the TS region of NaBr.

study the dynamics of the state created by an ultrashort laser pulse and to understand in detail how the excited bound NaI molecule (which we call here "transition state" (TS) to emphasize its role in the dissociation process) evolves in time and decays into products.

In this Letter we present quantum calculations of the behavior of the state created by the pump pulse. In these calculations a number of features and trends relevant to the experiments are considered. These are: (1) the simulation of the LIF signal for the transient on-resonance (free atom detection) and off-resonance (transition state) detection; (2) the prediction of the oscillation frequency and its dependence on the pump frequency; (3) the simulation of the decay and spread of the temporal oscillations; (4) the effect of thermal vibrational excitation in the ground state; (5) the dependence of the "transition state" dynamics on the shape and duration of the pump pulse; and (6) the changes observed in going from NaI and NaBr. We also show that the main results of the quantum calculations can be obtained by a semiclassical analysis which is simpler and usable for systems with several degrees of freedom.

2. The calculation

We assume that the experiment can be described in terms of a neutral electronic state $|1\rangle$ and an ionic state $|2\rangle$. The repulsive part of the potential energy $V_1(R)$ of the nuclei in the neutral state is that constructed by van Veen et al. [3,4] (the Ω =0⁺ state); to fit the absorption spectrum. The potential energy $V_2(R)$ of the ionic state is that used by Faist and Levine [5]. Both curves are shown in fig. 2.

The coupling $V_{12}(R)$ between the diabatic states $|1\rangle$ and $|2\rangle$ is

$$V_{12}(R) = A \exp[-\beta (R - R_x)^2]$$
 (1)

with A = 0.055 eV, $\beta = 0.69$ Å⁻¹ and $R_x = 6.93$ Å. The choice of β is arbitrary, however, the results are insensitive to it. R_x is the point where $V_1(R)$ and $V_2(R)$ cross and A was chosen so that the minimum gap between the adiabatic states has the value 0.11 eV given by Grice and Herschbach [6]; this value is also consistent with experiments [2,4].

We calculate the state [7] (see 2nd Ed. of ref. [7], eq. (5.145); see also ref. [8]. eq. (2.9'))

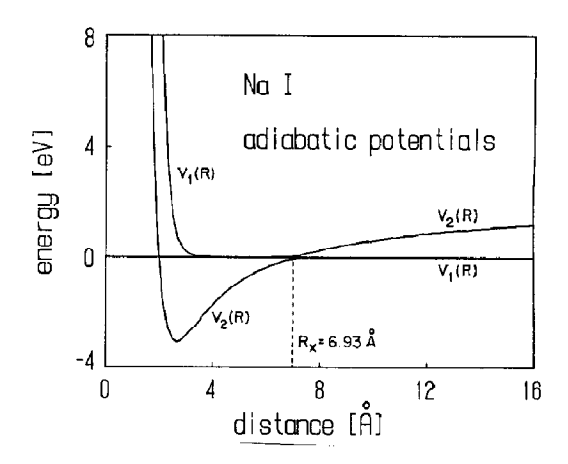


Fig. 2. The adiabatic potential energy surfaces. The difference between the adiabatic and diabatic surfaces is barely visible on the scale of this graph. The literature value of R_x is 6.93 Å. Our potentials give 7.01 Å.

$$|\Psi(t)\rangle = (+i\hbar) \int_{0}^{t} dt_{1} U(t-t_{1})$$

$$\times \mu \cdot E(t_{1}) |\Phi_{i}\rangle \exp(-iE_{i}t_{1}/\hbar)$$
(2)

created by the pump pulse. Here $|\Phi_i\rangle$ is the initial nuclear state, E_i is its energy, and μ is the transition dipole to the neutral state. The propagator $U(t) = \exp(-iHt/\hbar)$ contains the molecular Hamiltonian H describing the nuclear motion on the two coupled electronic states. The electric field vector is

$$E = E_0 \exp(-i\omega_0 t) \exp[-\alpha (t - t_0)^2], \tag{3}$$

where E_0 is a constant vector, $t_0 = 80$ fs, ω_0 is the frequency of the pulse and $\alpha = 1.1 \times 10^{-3}$ fs⁻²; the latter was chosen so that the full width at half maximum is 50 fs. We wrote only the term in E leading to absorption.

Since the transition dipole is unknown we take it to be constant (the Condon approximation). Furthermore, since the intensity measurements are not absolute we can give the constant multiplying $|\Psi(t)\rangle$ an arbitrary value.

In the quantum calculations the effects of the rotational motion are omitted *i for simplicity. It should be noted that at 600°C the initial rotational thermal energy is comparable to that of the initial

^{*1} They could be included as in ref. [9].

vibrational energy. In semiclassical calculations (see below) the two energies have small but comparable effects on the ensuing dynamics.

The only difficulty in calculating $|\Psi(t)\rangle$ is the evaluation of $U(t-t_1)$. This is done with a method described in detail by Avarellos and Metiu [10].

In what follows we assume that the laser-induced fluorescence is proportional to the population created by the pump pulse. To calculate this population we note that the wavefuntion $|\Psi(t)\rangle$ has the form

$$|\Psi(t)\rangle = \chi_1(R;t) |1\rangle + \chi_2(R;t) |2\rangle. \tag{4}$$

 $\chi_1(R; t)$ and $\chi_2(R; t)$ (here R is the Na-X distance, with X=I or Br) are the neutral and the ionic nuclear wavefunctions. We use them to define the populations

$$P_{b}(t) = \int_{0}^{R_{x}} dR |\chi_{1}(R;t)|^{2}$$
 (5)

and

$$P_{\rm f}(t) = \int_{R_{\rm b}}^{\infty} dR |\chi_{1}(R;t)|^{2}$$
 (6)

 $P_{\rm b}(t)$ gives the fraction of excited molecules which are in the neutral state and whose interatomic distance R is smaller than the crossing point $R_{\rm x}$. Even though R could be large ($R_{\rm x} = 6.93$ Å), the sodium atom in these molecules is neutral and is bound. $P_{\rm r}(t)$ is the fraction of molecules that are irreversibly dissociated and therefore it is the population of the free Na atoms.

The ionic population is

$$P_{i}(t) = \int_{0}^{\infty} dR |\chi_{2}(R;t)|^{2}.$$
 (7)

This population includes only those molecules (in the statistical ensemble) that have reached the ionic state via transitions from the neutral one; the ground state population is not included. These definitions are based on the diabatic picture, in the absence of the interaction V_{12} , and are therefore approximate.

We have also made some semiclassical calculations, using a recent model of Marcus [11] of a wave packet, consisting of a Gaussian distribution of energies in the packet and not necessarily to a Gaussian distribution in coordinate space, R. The individual wavefunctions used are in an angle representation and action—angle variables are thereby employed [12]. In this model, the frequency of oscillation of the packet is found to be the classical frequency of the motion at the most probable quantum number of the packet and so corresponds to the spacing of successive energy levels in the excited state at that energy, even though the analysis involves many states. This relation between spacing of successive levels at the most probable energy and the oscillation frequency of the wave packet was already realized in refs. [1,2]. In the following Letter [11] it is shown that for the pulse given in eq. (3)

$$\Psi \Psi^*(w,t) = \exp[-(w - v_0 t)^2 / \sigma_w^2]$$
 (8)

and

$$\sigma_w^2 = \nu_0^2 / \alpha$$
 (in the prespreading regime), (9)

where w is the angle variable (phase of the vibration in time divided by the period) and ν_0 is the oscillation (most probable) frequency of the packet. The oscillatory behavior results from noting that $w-\nu_0 t$ is defined to lie in the interval 0 to 1. The full width at half maximum, fwhm, in w space is $2\sqrt{\ln 2} \, \sigma_w$. To obtain the width in time we simply invoke ν_0 , so yielding $2\sqrt{\ln 2} \, \sigma_w/\nu_0$. In the flat region of $V_1(R)$ potential (for $R < R_x$), then the fwhm in the R space is simply $2\sqrt{\ln 2} \, \sigma_w \nu_R/\nu_0$, where ν_R is the "local" velocity of the system at R.

3. Results

In fig. 3 we show the population of the bound (i.e. $P_b(t)$) and free (i.e. $P_f(t)$) Na together with the experimental transients obtained by TS detection [1,2]. Note the resemblance between $P_b(t)$ and the off-resonanc LIF signal as well as that of $P_f(t)$ with the onresonance signal. This suggests that to a reasonable approximation the experiments measure $P_b(t)$ and $P_f(t)$. The time constants of oscillations and plateaus in the experimental results are similar to those of the bound and free populations: the peak positions of the observed oscillations are very close to the computed ones, but the widths are larger.

There are several factors which should be considered: (1) The LIF signal is roughly proportional to

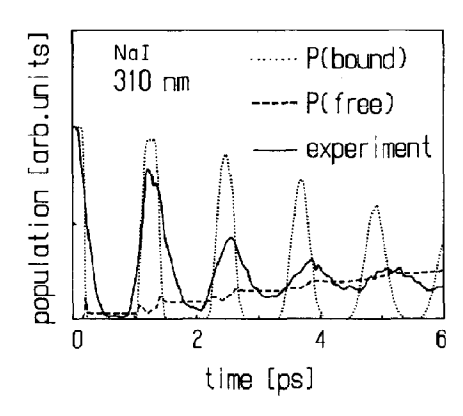


Fig. 3. The bound and free neutral population and the observed LIF signal. We used a Gaussian pump pulse with a wavelength of 310 nm and half width at half maximum of 50 fs. The initial state was v=0.

the duration of the probe pulse ($\approx 100 \text{ fs}$); it should be compared to an integral of $P_{\rm b}(t)$ over a time interval equal to the duration of the probe pulse and centered at the time when the pulse intensity has its maximum. (2) $P_b(t)$ should be thermally averaged over the initial vibrational and rotational states; when this is done the peaks become broader (see below). (3) The decay of the peak heights in the LIF signal is faster than that of $P_{\rm b}(t)$, but the two can be made very close by decreasing slightly the value of A in eq. (1). (4) The coupling $V_{12}(R)$ in the crossing region may have different parameters from those of eq. (1). (5) We assumed that the transition dipole μ involved in the excitation by the probe pulse is constant for $R < R_x$ and zero for $R > R_x$. Other dependence of μ on R will change the LIF signal. (6) We have not considered in detail the spatial overlap of the pump-probe pulses, which can affect the temporal shape of the LIF signal.

The results in fig. 3 are for a pump wavelength of 310 nm. Rosker, Rose and Zewail [2] also reported measurements with the pump wavelengths of 300 and 328 nm, and showed that the time constants for the TS detection depend on the excitation wavelength. Our calculations (not shown here) reproduce this dependence.

Note that the time evolution of the free population resembles the on-resonance signal shown in fig. 1. The only discrepancy is at the shortest time when the measured signal is higher than the computed one. We assume that this difference is due to the purely re-

pulsive $\Omega=1$ neutral state [3] which was not included in these calculations.

The experiments were carried out at 600° C and the v=1 and v=2 vibrational states of the electronical ground state were substantially populated. We have calculated $P_{\rm b}(t)$ and $P_{\rm f}(t)$ for the initial states v=1 and v=2 and found that they look similar to the populations for v=0 (fig. 3), except that the peaks are broader and the position of the late peaks are slightly shifted to larger times. The thermal averages of $P_{\rm b}(t)$ and $P_{\rm f}(t)$ which include the v=0 through v=2 states resemble even more the experimental results than the values for v=0, and are expected to bear a closer resemblance when the rotational effects are included (see below).

We note that the importance of the v=1 and v=2 states depends on the pump wavelength. For $\lambda=310$ nm $P_b(t)$ for the initial state v=1 is about 75% of that for v=0; if $\lambda=328$ nm $P_b(t)$ for v=0 is 7.5 times larger than $P_b(t)$ for v=1.

By computing the populations created by Gaussian and square pulses of the same temporal width (50 fs) we find that the pulse shape does not play a major role: the energy distributions of the state created by the two different pump pulses are slightly different, but this causes only *minor* changes in the shape of $P_b(t)$ and $P_f(t)$. These changes are well within the experimental error. We believe that for shorter pulses (e.g. 10 fs) different temporal shapes could lead to different signals.

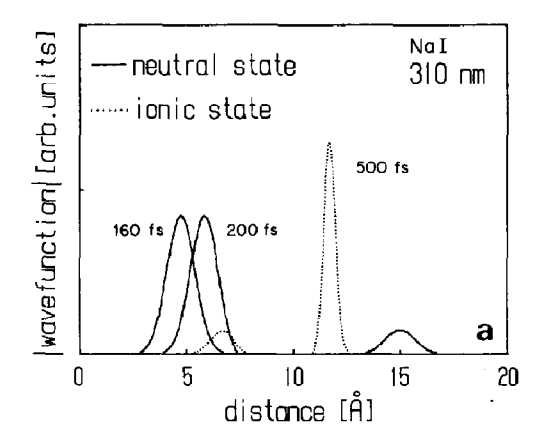
The dependence of $P_{\rm b}(t)$ and $P_{\rm f}(t)$ on the temporal width of the pulse is dramatic. For a 9 fs square pulse the peaks of $P_{\rm b}(t)$ are much broader and the heights of the successive peaks go to zero much earlier than for the 50 fs pulse.

We have also performed calculations for the NaBr molecule using the potential energy information contained in refs. [3-5,7,8,13], and found that the evolution of $P_b(t)$ tracks the LIF signal shown in fig. 1. The main cause for the difference between the NaI and NaBr signals is that the V_{12} coupling for NaBr is smaller and thus most of the neutral wave train remains on the neutral state and leads to irreversible dissociation.

The fact that the time evolution of the neutral bound population tracks so faithfully that of the detected signal gives a strong evidence (see also refs. [1,2]) regarding the physical reason for the observed

signal oscillations. In the TS region the probe pulse can excite the bound sodium to NaI* as long as the molecule is in the neutral state; no such excitation is possible if the molecule is in the ionic state and the interatomic distance is large. Thus if the wavefunction is spatially narrow it can oscillate from being almost completely ionic to being almost completely neutral; the molecule alternates from being capable of absorbing the probe photons, and therefore giving a fluorescence signal, and being incapable of such absorption; the fluorescence signal reflects this alternating motion between a spectroscopically bright (neutral) and spectroscopically dark (ionic) state.

This insight is confirmed by further calculations. In fig. 4a we show the neutral $|\chi_1(R; t)|^2$ and ionic $|\chi_2(R; t)|^2$ diabatic wavefunctions at several im-



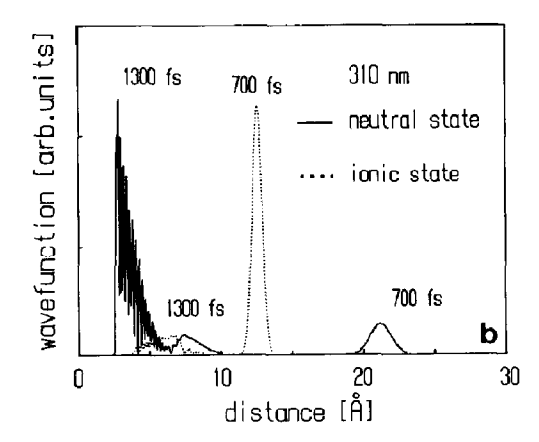


Fig. 4. The absolute value of the diabatic nuclear wavefunctions for the excitation conditions of fig. 3, at five different times. (a) The results for 160, 200 and 500 fs; (b) the results for 700 and 1300 fs.

portant times. The full line curve at left shows $|\chi_1(R;t)|^2$ for t=160 fs. At this time the intensity of the Gaussian pulse is practically zero (the pulse is centered at $t_0=80$ fs and has a full width at half height of 50 fs). No ionic component has been created at this time. At 200 fs the neutral wavefunction has moved towards and overlaps with the crossing point, and a small ionic component has been created. Note that this is exactly the time when $P_b(t)$ first starts going down (fig. 3). At 500 fs most of the population is ionic and the only neutral population consists of free Na. At this time no TS absorption occurs because the excitation energies of Na⁺, I⁻ or free sodium are all outside the reach of the off-resonance probe pulse.

At 700 fs (fig. 4b) the free Na wave packet is at 22 Å and the ionic state is moving towards the crossing point. At 1300 fs the neutral wavefunction hits the repulsive wall of $V_1(R)$; the wild spatial oscillations are typical for wavefunctions interacting with a sharp repulsive potential. At the same time (i.e. 1300 fs) we can still observe an ionic component in the crossing region.

Since the shape of the LIF signal depends on the fact that the wave train is narrow for the duration of the experiment, it is important to understand what determines the width of the wavefunction.

We can understand the width of the neutral state at 160 fs in fig. 4a, by examining eq. (2). The integral in eq. (2) can be written as a sum over the discrete time variable $n\tau$, where n is an integer and τ is a small time step. This way of writing displays the fact that the function $|\Psi(t)\rangle$ is a sum of amplitudes, one for each time step; the amplitude corresponding to $n\tau$ gives the state of the molecule at time t, if the photon was absorbed at $n\tau$. Eq. (2) tells us that since we do not know when the photon is absorbed we must add the amplitudes corresponding to all possible absorption times. The amplitude (i.e. the wavefunction) corresponding to absorption at $n\tau$ is the ground vibrational state propagated on the upper surface betwen $n\tau$ and t; this is a Gaussian wave packet slightly distorted by the motion. The state $|\Psi(t)\rangle$ is a sum of such packets and could be described as a "wave train". We introduce this name to emphasize that $|\Psi(t)\rangle$ for the present pulsed experiment differs from the wave packet used in Heller's theory of cw absorption cross section [13]. The spatial extent of $|\Psi(t)\rangle$ is much greater than that of the ground state wavefunction and it goes up with the length of the pulse. In our calculation the typical width of the "train" is around 1.5 Å (at 163 fs, see fig. 4).

The fact that the wave train narrows as it moves on the potential surfaces may seem contrary to the common expectation that with the passage of time such packets tend to disperse. Experience shows [14] that some potential energy surfaces can "focus" the wave packet approaching them. A simple semiclassical interpretation is given below.

We turn next to semiclassical calculations. Using the mean energy of the wave packet (available energy) the time of oscillation of the semiclassical wave packet was found to be about 1.3 ps, which agrees to about 5% with the value estimated from the first oscillation in fig. 3. This time was obtained from the integral $2\int dR/v_R$ between the turning points R_a and $R_{\rm b}$. Further, the semiclassically calculated ratio for the time when the system is probed in the bound neutral region to the total period in this first oscillation (equal to 0.22) is also close to that roughly estimated from fig. 3. Also, using eqs. (8) and (9) we can calculate the width of the packet in the R space. The quantum calculation for excitation at 328 nm gives widths of 1.3, 0.83 and 0.32 Å when the fwhm of the pump pulse was 50, 30 and 10 fs, respectively. These values agree with the semiclassical values of 1.6, 0.96 and 0.32 Å.

An increase of vibrational energy by amounts of $\hbar\omega$ and $2\hbar\omega$ ($\frac{1}{2}\hbar\omega$ being the ground state zero-point vibrational energy) increased the oscillation period by 4.3% and 9.0%, respectively. A comparison with the changes roughly estimated from quantum mechanical wave packet plots (not shown here) shows them to have roughly comparable increases. However, any detailed such comparison requires a knowledge of the quantum number distribution for each quantum mechanical packet.

At the temperature of the experiment (600°C) , the vibration of NaI in the ground electronic state is almost classical $(\hbar\omega/2k_{\text{B}}T\approx0.2)$ and its average energy is thus comparable with the average rotational energy, $k_{\text{B}}T$. When a rotational energy of this amount was added, the semiclassically calculated period of the oscillation increased by about 11%. The rotational energy provides a centrifugal potential which becomes small near the right-hand turning point. It

permits, thereby, the system to spend a longer time at large R's, and so increases the period of the motion.

We turn finally to the narrowing of the wave packet when the packet moves from its covalent to its ionic form at times short enough that spreading is still relatively minor. As seen in fig. 4b the width for the ionic form decreases to about 1/3 of its covalent value for the distances given there. The width in coordinate space ΔR is $v\Delta t$, where Δt is the width in time (initially about 50 fs) and v is the local velocity. The semiclassical wave packet described in the following Letter [11] has a prespreading width corresponding to a constant width in time space (50 fs). Thus, when, as for the two distances in fig. 4b, the velocity decreases to about 1/3 of its value the width ΔR is expected to decrease also to about 1/3, in agreement with the results in fig. 4b. Again, in the covalent region the classical velocity was about 0.032 Å/fs. Since the width in time space is 50 fs the semiclassically calculated width ΔR is about 1.6 Å, consistent with the result in fig. 4b.

A discussion of the subsequent spreading effect involves, in part, an analysis of the quantum mechanical wave packet in terms of its distribution in quantum number space, as noted earlier, and will be given later.

4. Conclusions

The present quantum and semiclassical calculations show the striking oscillatory behavior of the LIF signals generated during the dissociation of NaI and NaBr. As discussed in refs. [1,2], the TS signal oscillates because the molecule alternates between being neutral or ionic, and absorbs the probe pulse only in the neutral state. The oscillations are initially sharp (i.e. the troughs are deep) because the wave train created by the pulse is narrower than the spatial regions where the molecule is ionic or neutral. The sharpness is maintained in time because the wave train is not dispersed; it is, in fact, refocused whenever it approaches a turning point at large R, for reasons discussed semiclassically in section 3. The long time decay of the signal is due to the irreversible dissociation of the molecules to form free Na.

The plateaus in the on-resonance LIF signal appear whenever the narrow wave train passes through

the crossing region and there is a slight increase (integrated burst) in the free sodium population. If the probe laser pulse were substantially wider, the wave train would be broader and the free Na population would seem to increase continuously.

Naively one might think that the time resolution (i.e. the sharpness of the oscillations) in this kind of experiment could be improved by using shorter pulses. We find that if the temporal width of the pulse is too small, the energy distribution of the excited states is much broader, the motion of the wave train has a greater variety of time scales, and this leads to its rapid dispersion and faster dephasing. In the other extreme, if the pulse is long the energy distribution of the wave train created by it is narrow, but its spatial extent is large. In that case the train cannot alternate between being completely neutral and completely ionic; this will increase the background signal, suppress the dips between the peaks and again diminish the time resolution.

Acknowledgement

At Santa Barbara this work was supported by the National Science Foundation Grant CHE87-13619 and in part by the Office of Naval Research. The work

at Caltech was supported by AFOSR through Grant No. 87-0071 (AHZ) and by the National Science Foundation (RAM).

References

- [1] T.S. Rose, M.J.Rosker and A.H. Zewail, J. Chem. Phys. 88 (1988) 6672.
- [2] M.J. Rosker, R.S. Rose and A.H. Zewail, Chem. Phys. Letters 146 (1988) 175.
- [3] N.J.A. van Veen, M.S. de Vries, J.D. Sokol, T. Baller and A.E. de Vries, Chem. Phys. 56 (1981) 81; N.J.A. van Veen, Dissertation, Amsterdam, The Netherlands (1980).
- [4] S.H. Schaefer, D. Bender and E. Tiemann, Chem. Phys. 89 (1984) 65; Chem. Phys. Letters 92 (1982) 273; J. Chem. Phys. 78 (1983) 6341.
- [5] M.B. Faist and R.D. Levine, J. Chem. Phys. 64 (1976) 2953.
- [6] R. Grice and D.R. Herschbach, Mol. Phys. 27 (1974) 159.
- [7] R. Loudon, The quantum theory of light (Clarendon Press, Oxford, 1973) p, 279.
- [8] S.Y. Lee and E.J. Heller, J. Chem. Phys. 71 (1979) 4777.
- [9] V. Engel and H. Metiu, J. Chem. Phys. 89 (1988) 1986.
- [10] J. Alvarellos and H. Metiu, J. Chem. Phys. 88 (1988) 4957.
- [11] R.A. Marcus, Chem. Phys. Letters 152 (1988) 8.
- [12] R.A. Marcus, Chem. Phys. Letters 7 (1970) 525; J. Chem. Phys. 54 (1971) 3965.
- [13] E.J. Heller, J. Chem. Phys. 68 (1978) 3891.
- [14] R. Heather and H. Metiu, Chem. Phys. Letters 118 (1985)